Available online at www.sciencedirect.com
SCIENCE DIRECT®
Journal of Nuclear Materials 349 (2006) 133–149
journal of nuclear materials
www.elsevier.com/locate/jnucmat

Diffusivity, activity and solubility of oxygen in liquid lead and lead–bismuth eutectic alloy by electrochemical methods

Rajesh Ganesan [a], T. Gnanasekaran [a,*], Raman S. Srinivasa [b]

[a] *Liquid Metals and Structural Chemistry Division, Chemistry Group, Indira Gandhi Centre for Atomic Research, Kalpakkam 603 102, Tamil Nadu, India*

[b] *Department of Metallurgical Engineering and Materials Science, Indian Institute of Technology Bombay, Mumbai 400 076, India*

Received 17 May 2005; accepted 28 October 2005

Abstract

The diffusivity of oxygen in liquid lead and lead–bismuth eutectic (LBE) alloy was measured by a potentiostatic method and is given by $\log(D_O^{Pb}/\text{cm}^2\,\text{s}^{-1}) = -2.554 - 2384/T$ (± 0.070), 818–1061 K, and $\log(D_O^{LBE}/\text{cm}^2\,\text{s}^{-1}) = -0.813 - 3612/T$ (± 0.091), 811–980 K. The activity of oxygen in lead and LBE was determined by coulometric titration experiments. Using the measured data, the standard free energy of dissolution of oxygen in liquid lead and LBE was derived and is given by

$$G^{xs}_{O(Pb)} = -121\,349 + 16.906T\ (\pm 560)\text{J(g atom O)}^{-1}, \quad 815\text{–}1090\ \text{K},$$

$$G^{xs}_{O(LBE)} = -127\,398 + 27.938T\ (\pm 717)\text{J(g atom O)}^{-1}, \quad 812\text{–}1012\ \text{K}.$$

Using the above data, the Gibbs energy of formation of PbO(s) and equilibrium oxygen pressures measured over the oxygen-saturated LBE alloy, the solubility of oxygen in liquid lead and LBE were derived. The solubility of oxygen in liquid lead and LBE are given by $\log(S/\text{at.\%O}) = -5100/T + 4.32$ (± 0.04), 815–1090 K and $\log(S/\text{at.\%O}) = -4287/T + 3.53$ (± 0.06), 812–1012 K respectively.

1. Introduction

Liquid lead and lead–bismuth eutectic (LBE) alloy (44.1 at.% Pb and eutectic temperature of 398 K) are the candidate coolant materials for accelerator driven systems (ADS) as they can also serve as spallation targets to produce high-energy neutrons [1]. LBE has been extensively used as a coolant in compact nuclear reactors of submarines in Russia [2]. Because of their low chemical reactivity, Pb and LBE are proposed for use as coolant in advanced fast breeder reactors [3]. These coolants are highly corrosive towards structural steels, but this corrosion can be minimised by suitable control of the oxygen potential in the coolant and thereby forming a protective oxide layer on the steels [2]. Oxygen control systems (OCS), which essentially

* Corresponding author. Tel.: +91 44 2748 0302; fax: +91 44 2748 0065.
E-mail address: gnani@igcar.ernet.in (T. Gnanasekaran).

0022-3115/$ - see front matter © 2005 Elsevier B.V. All rights reserved.
doi:10.1016/j.jnucmat.2005.10.006

employ a mixture of hydrogen and water vapour with argon carrier gas, are used for this purpose [4]. The time scale of the oxygen control process via OCS is determined by the kinetics of reaction of the gases with liquid metals and by the diffusivity of oxygen in liquid metal. Nature and extent of formation of the oxide layer on structural steels would depend on the thermochemistry of oxygen in the coolant in addition to the nature of processes on the steel–coolant interface. As part of our studies [5–7] on the chemical behaviour of oxygen in lead, bismuth and LBE, the diffusivity, activity and solubility of oxygen in liquid lead and LBE have been measured by electrochemical methods and are described in this work.

2. Literature review

2.1. Pb–O system

The diffusivity of oxygen in liquid lead has been measured by several investigators [8–14]. Details of the electrochemical techniques employed, the results obtained and the temperature range of measurements in these works are listed in Table 1. Recently Zhang and Li [3] have estimated the diffusivity of oxygen in lead based on the Stokes–Einstein relation. As it is seen from the table, a considerable discrepancy exists among the reported data, and data at temperatures below 973 K are not available.

The activity of oxygen in liquid lead and hence $G^{xs}_{O(Pb)}(= RT \ln \gamma_O)$ has been measured by several authors [11,14–22] using electrochemical methods, the details of these literature data are given in Table 2. In these works, the oxygen concentration in liquid lead has been varied either by adding a known amount of PbO or by coulometric titration of oxygen into liquid lead. Henry's law was assumed to be valid up to the saturation limit of oxygen in lead by the majority of the research workers except by Charle and Osterwald [14] and Isecke [18].

The solubility of oxygen has been measured in the past mainly by two methods, viz., sampling and electrochemical methods. The sampling method is an age-old method. Although literature data based on the sampling method exist from the last century, the method suffers from large uncertainty due to possible inclusion of Pb or impurity oxides in the lead oxide taken for analysis [23]. Literature data on the solubility of oxygen in liquid lead

Table 1
Literature data on the diffusivity of oxygen in liquid lead

S. no.	Electrochemical cell	Method	Diffusivity ($cm^2\ s^{-1}$) $D = D_0 \exp(-E^*_a/RT)$		Temp. range (K)	Diffusivity ($cm^2\ s^{-1}$)		Author and Year
			D_0 ($cm^2\ s^{-1}$)	E_a ($J\ mol^{-1}$)		1075 K	1175 K	
1	Solid electrolyte emf method using CSZ	Potentiostatic	[a]6.32×10^{-5}	[a]14979	973–1173	1.18×10^{-5}	[b]1.36×10^{-5}	Arcella and Fitterer, 1968 [8]
2	SS, $[O]_{Pb}$ |CSZ| Ni, NiO, SS	Potentiometric	[a]1.29×10^{-5}	–	1023 (single point)	–	–	Bandyopadhyay and Ray, 1971 [9]
3	Ir, $[O]_{Pb}$ |CSZ| Ni, NiO, Pt	Potentiometric	$(9.65 \pm 0.71) \times 10^{-5}$	20083 ± 6067	1073–1373	1.02×10^{-5}	1.23×10^{-5}	Honma et al., 1971 [10]
4	Chromel, $[O]_{Pb}$ |CSZ| air, Pt	Potentiostatic	$(1.44^{+0.46}_{-0.34}) \times 10^{-3}$	25941 ± 2803	1012–1353	7.90×10^{-5}	1.01×10^{-4}	Szwarc et al., 1972 [11]
5	$[O]_{Pb}$ |CSZ| Ni, NiO or Mo, MoO_2	Galvanostatic	[a]1.30×10^{-5}	–	1063 (single point)	–	–	Kawakami and Goto, 1973 [12]
6	Nichrome, Pt, Ni, NiO |CSZ| $[O]_{Pb}$ |CSZ| FeO, Fe_3O_4, SS	Combined potentiostatic and potentiometric techniques	$(1.48^{+0.62}_{-0.44}) \times 10^{-3}$	19497 ± 10711	1153–1408	[b]1.67×10^{-4}	2.01×10^{-4}	Otsuka and Kozuka, 1975 [13]
7	Ir, $[O]_{Pb}$ |stab.ZrO_2| air, Pt	Potentiometric or galvanostatic	[a]1.90×10^{-3}	[a]20920	1173–1323	[b]1.83×10^{-4}	2.23×10^{-4}	Charle and Osterwald, 1976 [14]

[a] Error not given.
[b] Extrapolated data.

Table 2
Literature data on the activity of oxygen in liquid lead

S. no.	Electrochemical cell	Method	$G^{xs}_{O(Pb)}$ (J (g atom of O^{-1}))	Temp. range (K)	Author and year
1	Ir, $[O]_{Pb}$ |MgSZ| Cu, Cu_2O, Pt Ir, $[O]_{Pb}$ |YDT| Ni, NiO, Pt	Coulometric titration (constant current mode)	$G^{xs}_{O(Pb)} = (-119411 \pm 2636) + (14.222 \pm 3.138)\,T$	783–973	Alcock and Belford, 1964 [15]
2	Pt, $[O]_{Pb}$ |Stabilised zirconia| air, Pt	Emf technique	[a] $G^{xs}_{O(Pb)} = -106395 + 10.254\,T$	903–1253	Fischer and Ackermann, 1966 [16]
3	Pt, Ir, $[O]_{Pb}$ |CSZ| Ni, NiO, Pt	Emf technique Oxygen added in the form of PbO	$G^{xs}_{O(Pb)} = -101002 \pm 628$	1373	Jacob and Jeffes, 1971 [17]
4	Chromel, $[O]_{Pb}$ |CSZ| air, Pt	Coulometric titration (potentiostatic)	[a] $G^{xs}_{O(Pb)} = -105855 + 18.661\,T$	1012–1353	Szwarc et al., 1972 [11]
5	Ir, $[O]_{Pb}$ |CSZ| air, Pt	Emf technique Oxygen added in the form of PbO	[a] $G^{xs}_{O(Pb)} = -119840 + 15.794\,T$	1173–1373	Charle and Osterwald, 1976 [14]
6	Ir, $[O]_{Pb}$ |CSZ| air, Pt	,,	[a] $G^{xs}_{O(Pb)} = -120376 + 16.255\,T$	1173–1323	Isecke, 1977 [18]
7	Pt, Ir, $[O]_{Pb}$ |CSZ| air, Pt	,,	$G^{xs}_{O(Pb)} = -118600 + 14.1\,T$ (± 1300)	1073–1673	Otsuka and Kozuka, 1979 [19]
8	Pt/Cr-cermet $[O]_{Pb}$ |CSZ| O_2, Pt Pt, Ir, $[O]_{Pb}$ |CSZ| O_2, Pt	,,	[a] $G^{xs}_{O(Pb)} = -116717 + 12.699\,T$	1073–1203	Taskinen, 1979 [20]
9	Pt, Ir, $[O]_{Pb}$ |CSZ| air, Pt	,,	$G^{xs}_{O(Pb)} = -117170 + 12.9\,T$ (± 500)	1023–1273	Otsuka and Kozuka, 1981 [21]
10	Pt, Ir, $[O]_{Pb}$ |YSZ| air, Pt	,,	[a] $G^{xs}_{O(Pb)} = -105633$ and -106387	787	Ghetta et al., 2002 [22]

[a] Error not given.

Table 3
Literature data on the solubility of oxygen in liquid lead by electrochemical method

S. no.	Electrochemical cell	Method	$\log(S/\text{at.\%O}) = A - B/T$	Temp. range (K)	Author and year
1	Ir, $[O]_{Pb}$ |MgSZ| Cu, Cu_2O, Pt Ir, $[O]_{Pb}$ |YDT| Ni, NiO, Pt	Coulometric titration (constant current mode)	$4.53 \pm 0.14 - (5240 \pm 120)/T$	783–973	Alcock and Belford, 1964 [15]
2	Pt, Ir, $[O]_{Pb}$ |CSZ| Ni, NiO, Pt	Emf technique Oxygen added in the form of PbO	[a]3.08 at.%	1373 (single point)	Jacob and Jeffes, 1971 [17]
3	Chromel, $[O]_{Pb}$ |CSZ| air, Pt	Coulometric titration (potentiostatic)	[a]$3.87 - 5600/T$	1170–1353	Szwarc et al., 1972 [11]
4	Ir, $[O]_{Pb}$ |CSZ| air, Pt	Emf technique Oxygen added in the form of PbO	[a]$4.30 - 5055/T$	1173–1373	Charle and Osterwald, 1976 [14]
5	Ir, $[O]_{Pb}$ |CSZ| air, Pt	,,	[b]$4.49 - 5182/T$ (Std. dev. $= \pm 0.02$)	1173–1323	Isecke, 1977 [18]
6	Pt, Ir, $[O]_{Pb}$ |CSZ| air, Pt	,,	[b]$4.49 - 5170/T$ (Std. dev. $= \pm 0.02$)	1073–1118	Taskinen, 1979 [20]
7	Fe, $[O]_{Pb}$ |YSZ| O_2 (1 atm.), Pt	'Open top bubble' apparatus (oxygen added by injecting known amount of gas in pulse mode)	[b]$2.07 - 3007/T$ (Std. dev. $= \pm 0.02$)	728–879	Conochie et al., 1981 [24]

[a] Error not given.
[b] Fitted expression from their raw data.

determined by the electrochemical technique employing oxygen concentration cells and the experimental details are given in Table 3 [11,14,15,17,18,20,24]. In these works, the solubility has been determined either directly from the measured emf data and the amount of oxygen added coulometrically (for example by Alcock and Belford [15]) or from the Gibbs energy of solution of oxygen in lead and the standard molar Gibbs energy of formation of PbO (s) as a function of temperature (for example by Jacob and Jeffes [17]).

2.2. LBE–O system

Experimental data on the diffusivity of oxygen in liquid LBE have not been reported so far. Lefhalm et al. [25] indirectly derived the diffusion coefficient in stagnant LBE alloy at 703 K but the derived values are more than one order of magnitude higher than the corresponding values in pure lead and bismuth. Further, the diffusion coefficient was found to be dependent on the mass of LBE employed indicating the uncertainty in the results. Zhang and Li [3] estimated the diffusion coefficient of oxygen in LBE using the Stokes–Einstein relation.

Literature data on the activity [26–29] and solubility of oxygen in liquid lead–bismuth alloys [30–33] are limited. Taskinen [26] determined the oxygen activity in lead–bismuth alloys at 1103 K, 1133 K and 1173 K by an emf method. The author had measured the oxygen activity up to about 6 at.% bismuth in lead at 1103 K and 1133 K while the measurement at 1173 K was up to about 58 at.% bismuth in lead (cf. Bi content in LBE is 55.9 at.% Bi). Otsuka et al. [27] measured the oxygen activity in the entire composition range of the lead–bismuth alloy ($N_{Bi} = 0.10$, 0.25, 0.40, 0.50, 0.65, 0.80 and 0.90) at 1073 K. They had also measured the activity of oxygen in Pb–55at.%Bi at 1173 K. Anik and Frohberg [28] measured the oxygen activity in the entire Pb–Bi alloy composition range ($N_{Bi} = 0.1$ to 0.9 with an increment of 0.1) at 1173 K. Prabhakar and Kapoor [29] determined the activity coefficient of oxygen in Pb–Bi alloys with 0 to about 3 wt% bismuth in the temperature range of 913–1034 K. Data on the activity of oxygen in LBE at temperatures below 1000 K are not available.

Gromov et al. [30] reported the solubility of oxygen in LBE (widely called as Orlov expression) as, $\log(S/\text{mass\%O}) = -3400/T + 1.2$, 673–973 K, but the details of their experimental techniques are not available. Müller et al. [31] estimated the solubility of oxygen in liquid LBE using the corresponding data in the binary Pb–O and Bi–O systems and is given by

$$\log(S/\text{mass\%O}) = -4803/T + 2.52,\ 473\text{–}923\ \text{K}. \quad (1)$$

Recently Courouau [32] reported the solubility values based on the data obtained during the calibration of the electrochemical oxygen sensors used in LBE using $Bi–Bi_2O_3$ and $In–In_2O_3$ reference electrodes. Variation of the solubility data is given by

$$\log(S/\text{mass\%O}) = -4962/T + 3.3,\ 623\text{–}773\ \text{K}. \quad (2)$$

Ghetta et al. [33] had recently reported the solubility of oxygen in LBE by coulometric titration experiments but their experimental details are not available. The data reported by them is given by the following expression:

$$\log(S/\text{mass\%O}) = -4852/T + 3.28,\ 623\text{–}773\ \text{K}. \quad (3)$$

3. Experimental

Lead metal of 5 N purity (M/s. Strem Chemicals, USA) and bismuth metal of 4 N purity (M/s. Nuclear Fuel Complex, India) were used in this work. Ultra high-purity argon and synthetic air were used. The LBE alloy was prepared by melting a mixture of stoichiometric amounts of the metals in an alumina crucible under argon atmosphere glove box. The alloy was then sealed in a quartz ampoule under vacuum after initially purging the vacuum system with argon gas. The sample in the ampoule was equilibrated at 673 K for 4 days and then quenched in liquid nitrogen. The LBE alloy was characterized by studying its thermal behaviour using the DTA technique (M/s. Rheometric Scientific Co., UK).

One-end closed 15 mol% calcia stabilised zirconia (CSZ) solid electrolyte tube with round bottom (6 mm o.d., 4 mm i.d. and 150 mm long), supplied by M/s Nikkato Corporation, Japan was used for measurement of the diffusivity of oxygen in liquid lead and LBE. The electrochemical cell employed is represented by

$$\text{Kanthal, Ir, } [O]_{\text{Pb or LBE}} | \text{CSZ} | O_2 \text{ (0.21bar), Pt Cell-I.}$$

A cylindrical geometry was used for the measurements. The experimental arrangement of the cell is shown schematically in Fig. 1. The outer side of the electrolyte tube was coated with platinum paste (M/s. Eltecks Corporation, India) to a height of 40 mm. A small platinum wire mesh having a spot-welded platinum wire was co-fired with the coated Pt-paste and the Pt-wire served as the electrical lead for the reference side.

The lead metal or LBE alloy was taken inside the electrolyte tube such that on melting, the height of the molten metal column at 873 K matched exactly with the level of the outer electrode. Since iridium is compatible with both liquid lead and LBE, a short iridium wire (0.5 mm dia and 30 mm long, M/s. Goodfellow Cambridge Limited, England) spot-welded to a Kanthal wire was used as the electrical lead for the sample electrode. The thermo-emf due to dissimilar electrical leads, viz. Kanthal–platinum couple was measured and corrected for the cell emf. As the junction between Kanthal and iridium as well as junctions such as Ir–Pb or LBE, Pb or LBE–CSZ, CSZ–Pt were present in the constant temperature zone of the furnace, the thermo-emf due to these couples would not contribute to the cell output. Other details regarding the construction of the emf cell and experimental assembly are described elsewhere [5,6]. High purity argon gas passed over a purification train was used at the sample electrode. The purification train consisted of columns of regenerated LINDE 4A molecular sieves and active Cu impregnated $MgSiO_3$ pellets (popularly known as BASF catalyst, M/s. BASF Aktiengesellschaft, Germany) maintained at ambient temperature followed by columns containing metallic copper turnings at 500 °C, titanium sponge at 900 °C and calcium metal shots at 500 °C. Titanium taken in the form of a sponge, offered a large surface area leading to efficient purification. The outlet of the cell was again passed over another calcium metal column maintained at 500 °C. This was to avoid oxygen contamination due to back diffusion.

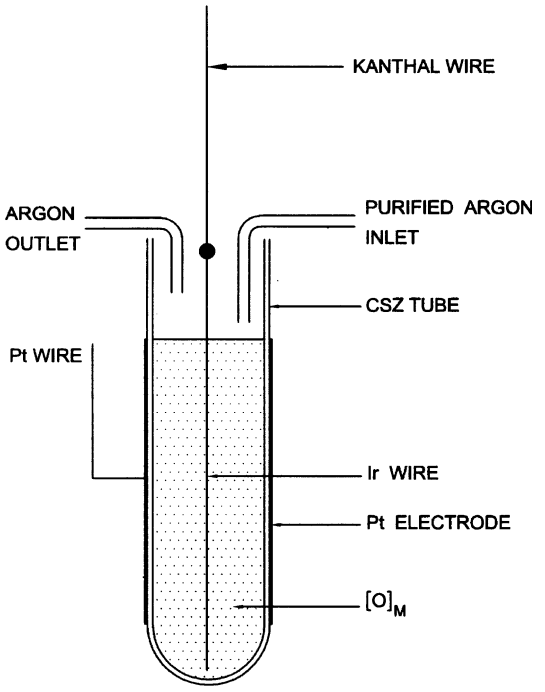

Fig. 1. Schematics of the experimental set-up used for measurement of the diffusivity of oxygen in liquid metal/alloy.

In this work, diffusivity measurements were made using a potentiostatic method, details of which have been described by Rapp and co-workers [34,35]. The electrochemical cell employed for diffusivity measurements can be represented as

$$\text{Kanthal, Ir, } [O]_{\text{Pb or LBE}} \underset{x=0}{|} \text{ Calcia Stabilised Zirconia } \underset{x=L}{|} O_2(0.21\text{ bar}), \text{Pt},$$

where L is the thickness of the electrolyte. At a constant temperature, the liquid metal in the cell containing dissolved oxygen, X_O^1, below its saturation limit was allowed to equilibrate. The cell output corresponding to the oxygen partial pressure P'_{O_2} dictated by this dissolved oxygen concentration at the experimental temperature was measured (E_1). A voltage E_2 ($= E_1 + \Delta E$) was then applied across the cell such that oxygen was pumped out from the liquid metal and instantaneously established an oxygen partial pressure of P''_{O_2}. An oxygen concentration lower than that at the start of the experiment would be established in the alloy at the inner electrode–electrolyte interface (X_O^2). Due to the concentration gradient of oxygen that is established between the liquid metal at this interface and in the bulk, a net flux of oxygen would set in. This flux of oxygen in the liquid metal can be followed by measuring the current in the external circuit as a function of time. If the kinetics of the oxygen ion transport through the electrolyte is rate limiting, polarization of the electrodes would occur. Under these conditions, a significant part of the applied jump voltage (ΔE) would be expended for the transport of O^{2-} ions through the electrolyte rather than being used by the diffusion process in the liquid

metal. This part of the potential is shown to be equal to $i_{ion}\Omega_{ion}$ [34] where i_{ion} is the ionic current through the electrolyte and Ω_{ion} is given by

$$\Omega_{ion} = \frac{1}{A}\int_0^{x=L} \frac{1}{\sigma_{ion}}\,dx, \tag{4}$$

where A is the area of the electro active surface of the solid electrolyte and σ_{ion} is the oxygen ion conductivity of the solid electrolyte which is related to the diffusion coefficient of the oxygen ion by Nernst–Einstein relation [36] as

$$\sigma_{ion} = \frac{n(Ze)^2 D_{ion}}{kT}, \tag{5}$$

where n is the density of defects, Ze is the charge of the conducting ion, D_{ion} is the diffusion coefficient of the ion, k is the Boltzmann constant and T is the temperature in Kelvin. The oxygen partial pressure at the electrode–electrolyte interface is related to applied potential as given below

$$E_2 - i_{ion}\Omega_{ion} = \frac{RT}{4F}\ln\frac{P'_{O_2}}{P''_{O_2}}. \tag{6}$$

For the experiment to be under true potentiostatic condition, i.e., to establish a time-independent P''_{O_2}, $i_{ion}\Omega_{ion}$ shall be small compared to E_2.

Diffusivity measurements were carried out in the pump-out mode by applying a jump voltage of 200 mV above the equilibrium emf value. The cell temperature could be controlled within ±0.5 K using a PID temperature controller. The emf of the cell was recorded using a high impedance electrometer (M/s. Keithley, model 6514 electrometer). For applying the jump voltage and measuring the resulting current a programmable source measure unit (M/s. Keithley, model 236 source measure unit) was used. The cell temperature was recorded using a data logger (M/s. Agilent Technologies, model 34970A data acquisition/switch unit). All these instruments were interfaced with a personal computer.

The activity of oxygen in liquid lead and LBE was measured as a function of oxygen concentration using a cell similar to the one used for determination of the diffusivity. A one end closed and flat bottomed calcia stabilised zirconia (CSZ) solid electrolyte tube (15 mol%CaO–ZrO_2, 13 mm o.d., 9 mm i.d. and 250 mm long), supplied by M/s Nikkato Corporation, Japan, was used for this study. The cell containing the liquid metal or alloy with unknown amount of oxygen (but below its saturation limit) was first allowed to equilibrate at a chosen temperature and the cell emf was measured. The oxygen concentration in the liquid metal or alloy was then varied by coloumetric addition or removal of oxygen. Typically 200–300 μA current was passed using the source measure unit for a time period ranging from 20 min to 3 h. The passage of current was generally carried out at a temperature chosen between 700 and 750 °C. After the passage of current, the cell temperature was changed and held at the experimental temperature for about 2 h till the emf became stable. The emf of the cell was then measured as a function of temperature. Measurements were carried out for several heating and cooling cycles. Generally the emf values became steady within 10 min after the cell temperature became stable. Before making the measurements, the stability of the cell output was monitored at least for 2 h at temperatures above 973 K and for at least 3–4 h at temperatures below 973 K. The readings were recorded when the emf values were stable within $\pm 5 \times 10^{-5}$ V.

Changes in concentration of oxygen in at.% in the metal/alloy after a coulometric titration can be calculated using the following expression:

$$\Delta X_O = X_{O(1)} - X_{O(2)} = 100 \cdot \left(\frac{M}{W}\right) \cdot \left(\frac{Q_{ion}}{2F}\right), \tag{7}$$

where $X_{O(1)}$ and $X_{O(2)}$ are oxygen concentrations in at.% before and after the passage of the electrical charge, respectively, M = molar mass of lead or LBE, W = mass of the metal or alloy, Q_{ion} = charge due to the passage of oxygen ion = $i_{ion}t$, i_{ion} = ionic current in Ampere and t = time in seconds.

4. Results and discussion

4.1. Oxygen in liquid lead

4.1.1. Diffusivity

At each experimental temperature, the current through the cell was measured as a function of time after application of a jump voltage. After attaining the steady state, a constant electronic current would only flow through the cell. The measured electronic current was subtracted from the total current to obtain the ionic current and the latter was used in Fig. 2 for determining the diffusion coefficient of oxygen (D_o) in the liquid metal. From the conductivity data of CSZ and the ionic current that were encountered in each experiment, the value of $i_{ion}\Omega_{ion}$ was calculated. This potential drop, arising due to kinetics of oxygen ion transport across the electrolyte was found to lie between 0.5 and 1.5 mV. Since

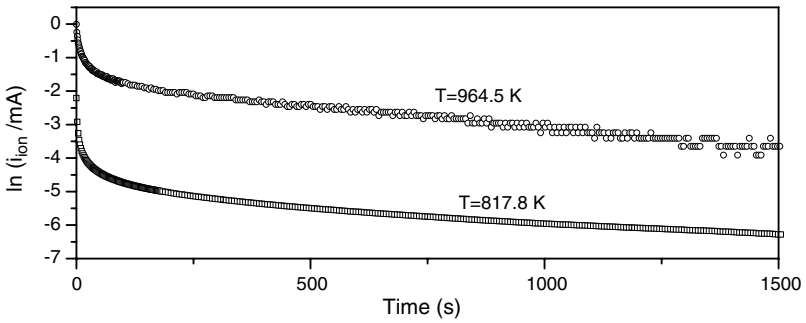

Fig. 2. Plots of $\ln i_{ion}$ vs. time derived using the measured cell current as a function of time during the potentiostatic experiments in the Pb–O system at 964.5 K ($E_1 = 976$ mV, jump voltage $\Delta E = 200$ mV) and 817.8 K ($E_1 = 747.3$ mV, jump voltage $\Delta E = 200$ mV).

these values are around 2 orders lower than the applied potential, the kinetics of oxygen ion transport through the electrolyte would not significantly influence the measurements of diffusivity of oxygen in liquid metal.

The diffusion of oxygen in the liquid metal electrode contained in the one-end closed cylindrical electrolyte tube is described by Fick's second law for cylindrical coordinates:

$$\frac{\partial X_o}{\partial t} = \frac{1}{r}\cdot\frac{\partial}{\partial r}\left(r\cdot D_o\cdot\frac{\partial X_o}{\partial r}\right), \tag{8}$$

where r = radial length (cm), X_o = oxygen concentration (in at.%) at the radial length 'r', D_o = diffusion coefficient of oxygen in the liquid metal ($cm^2\ s^{-1}$), t = time (s).

The boundary conditions for the system are given by

Applied potential	Concentration	Location	Time
–	X_O^1	$0 \leqslant r \leqslant a$	$t = 0$
(Cell emf $= E_1$)			
E_2	X_O^2	$r = a$	$t > 0$

where a is the inner radius of the electrolyte tube.

The general solution of Eq. (8) is given by the following expression [37]:

$$\frac{X_O^1 - X_O(r,t)}{X_O^1 - X_O^2} = 1 - \sum_{n=1}^{\infty}\frac{4}{\lambda_n^2}\cdot\exp\left(-\frac{D_o\lambda_n^2 t}{a^2}\right), \tag{9}$$

where $X_O(r, t)$ is the oxygen concentration in the liquid metal at time t and distance r from the center of the tube (radial length) and λ_n is the root of the Bessel function of 0th order. The term, $X_O^1 - X_O(r,t)$ (change in oxygen concentration) can be calculated from the amount of oxygen passed per unit volume. Thus, the above expression can be written as

$$\frac{\frac{1}{2F}\int_0^t i_{ion}\,dt}{\pi a^2 h(X_O^1 - X_O^2)} = 1 - \sum_{n=1}^{\infty}\frac{4}{\lambda_n^2}\cdot\exp\left(-\frac{D_o\lambda_n^2 t}{a^2}\right), \tag{10}$$

where i_{ion} = ionic current in Ampere, h = height of the liquid metal column in the electrolyte tube.

After differentiation and rearrangement of the resultant, the solution applicable after prolonged periods can be obtained as

$$i_{ion} = 8\pi h F D_O (X_O^1 - X_O^2)\exp\left[-\frac{(2.405)^2 D_O t}{a^2}\right]. \tag{11}$$

Typical plots of $\ln i_{ion}$ vs. t are shown in Fig. 2. The current data obtained 500 s after application of the jump voltage were used for deriving the diffusivity. The experimental parameters such as temperature, applied voltage and the derived diffusivity data are summarised in Table 4. The measured diffusion coefficients of oxygen in liquid lead are shown as a function of reciprocal temperature in Fig. 3 and the linear least-squares fitted expression to the measured data is given below

$$\log(D_O^{Pb}/\ cm^2\ s^{-1}) = -2.554 - 2384/T\ (\pm 0.070),\quad 818\text{–}1061\ K. \tag{12}$$

Diffusion coefficients reported in this work are data of their first kind for diffusivity at temperatures below 973 K. For comparison, data from literature are also shown in Fig. 3. Although the present data exhibit higher slope than those data reported in the literature, the data at high temperatures agree within ~0.2 orders of magnitude with the data reported

Table 4
Experimental results of oxygen diffusion measurements in the Pb–O system

T (K)	E_1 (mV)	E_2 (mV)	D_O ($cm^2\ s^{-1}$)
817.8	747.3	947.3	4.03×10^{-6}
868.8	731.9	931.9	4.99×10^{-6}
881.7	1046.0	1246.0	4.57×10^{-6}
964.5	976.0	1176.0	8.42×10^{-6}
1053.0	678.4	878.4	1.49×10^{-5}
1060.7	721.4	821.4	1.85×10^{-5}

by Bandyopadyay et al. [9], Kawakami and Goto [12] and low temperature data of Arcella and Fitterer [8] and Honma et al. [10].

The data estimated by Zhang and Li [3] by invoking the Stokes–Einstein equation are clearly very high compared to the rest of the data shown in Fig. 3. The data reported by Szwarc et al. [11], Otsuka and Kozuka [13] and Charle and Osterwald [14] are distinctly higher than the present data by approximately one order of magnitude. Szwarc et al. [11] had used chromel as the electrical lead. The components of chromel alloy, namely, Cr and Ni have significant solubilities in Pb [38] and their interaction with oxygen may affect the oxygen diffusivity. The reasons for the deviation of the values reported by Otsuka and Kozuka [13] and Charle and Osterwald [14] are not known.

4.1.2. Activity and solubility

The variation of the cell emf with temperature for different oxygen concentrations in liquid lead is shown in Fig. 4. For each oxygen concentration, a sharp change in slope is seen at a specific temperature indicating clearly the saturation and unsaturation regions.

The cell emf is related to the oxygen partial pressure at the sample electrode by the following expression:

$$-4E_1F = RT\ln p_{O_2(1)} - RT\ln p_{O_2(ref)}. \tag{13}$$

After the passage of current, the cell emf is related to the changed oxygen partial pressure as

$$-4E_2F = RT\ln p_{O_2(2)} - RT\ln p_{O_2(ref)}. \tag{14}$$

Assuming Henry's law to be valid up to saturation and by using the expressions (7), (13) and (14), the activity coefficient of oxygen in lead can be calculated as,

$$\gamma_{O(Pb)} = \frac{\Delta p_{O_2}^{1/2}}{\Delta X_O} = \frac{p_{O_2(1)}^{1/2} - p_{O_2(2)}^{1/2}}{X_{O(1)} - X_{O(2)}}. \tag{15}$$

Using the $\gamma_{O(Pb)}$ values, the activity of oxygen in the liquid metal can be calculated.

The solubility of oxygen in liquid metal can be derived by considering the following equilibrium:

$$1/2\,O_2 \Longleftrightarrow [O_{at.\%}]_{Pb}. \tag{16}$$

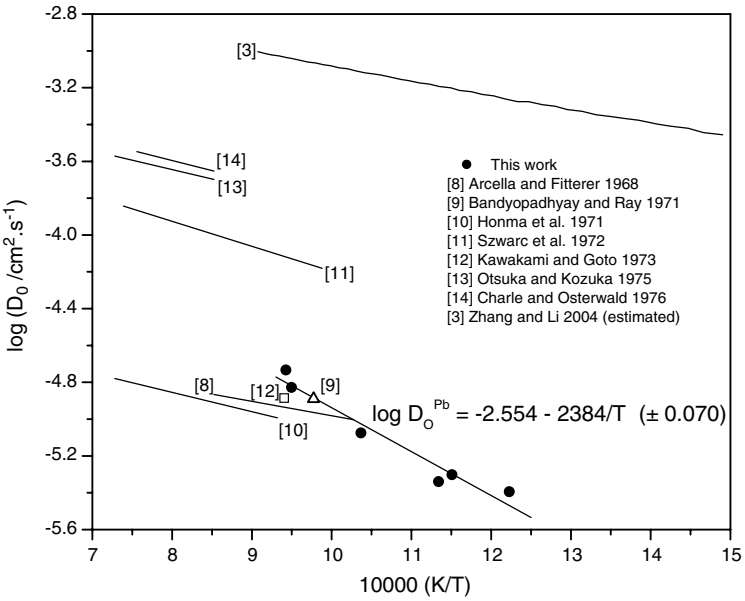

Fig. 3. Comparison of the diffusion coefficient of oxygen in liquid lead determined in this work with literature data.

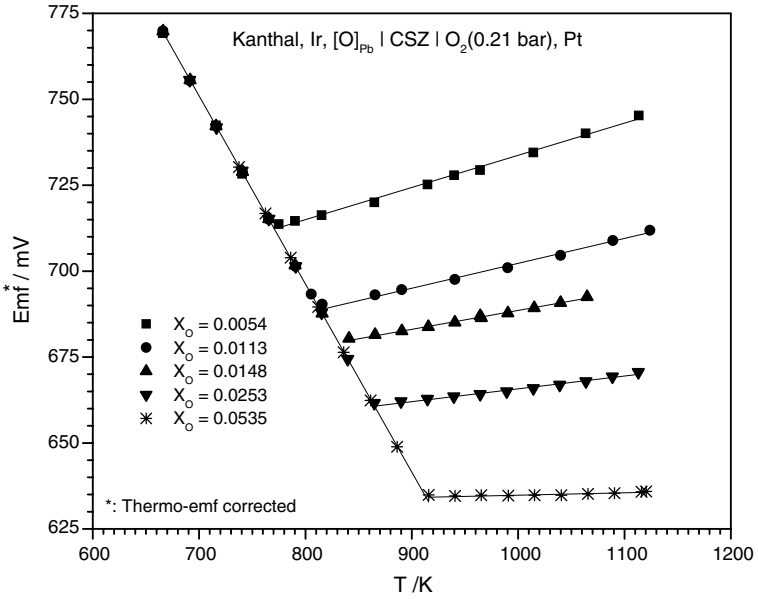

Fig. 4. Dependence of the emf on the cell temperature for different oxygen concentrations in liquid lead.

The Gibbs energy change for the above equilibrium is given by

$$\Delta G_R = -RT\ln K = -RT\ln\frac{a_O}{p_{O_2}^{1/2}} = -RT\ln\frac{X_O\cdot\gamma_{O(Pb)}}{p_{O_2}^{1/2}}. \quad (17)$$

By rearrangement, one gets,

$$RT\ln X_O = -RT\ln\gamma_{O(Pb)} + RT\ln p_{O_2}^{1/2} = -G^{xs}_{O(Pb)} + RT\ln p_{O_2}^{1/2}. \quad (18)$$

At saturation, metal oxide precipitates and hence $X_O = X_O^{sat} = S$, where S is the solubility of oxygen in the liquid lead which is given by

$$\ln(S/\text{at.\%O}) = \frac{G^{xs}_{O(Pb)}}{RT} + \ln(p_{O_2}^{sat})^{1/2}. \quad (19)$$

In the above expression, $p_{O_2}^{sat}$ corresponds to the Pb(l)–PbO(s) equilibrium. Thus, using the $G^{xs}_{O(Pb)}$ values and the equilibrium oxygen pressure, the solubility of oxygen in liquid lead can be determined.

Using the emf data for the unsaturated solutions of oxygen in liquid lead, $G^{xs}_{O(Pb)}$ values with respect to 1 at.% standard state were derived as a function of temperature and are plotted. The least-squares fitted expression for $G^{xs}_{O(Pb)}$ is given by,

$$G^{xs}_{O(Pb)} = -121349 + 16.906T\ (\pm 560)\ \text{J (g atom O)}^{-1},\quad 815\text{–}1090\ \text{K}. \quad (20)$$

The $G^{xs}_{O(Pb)}$ values are compared with those reported in the literature [11,14–22] in Fig. 5. It can be seen from the figure that the values from the present work are in close agreement with the majority of the reported data. The data reported by Szwarc et al. [11] and Fischer and Ackermann [16] deviate significantly from the rest of the data. It is to be noted that Szwarc et al. [11] had used chromel as electrical lead while Fischer and Ackermann [16] had employed platinum for this purpose. It is known that Pt and the components of chromel are not compatible with Pb [38]. Further, Fischer and Ackermann [16] had employed a voltmeter with low input impedance ($\approx 10^7\ \Omega$) for measuring emf of the cell while measuring devices with input impedance $>10^{12}\ \Omega$ are considered to be adequate for this service. Alcock and Belford [15] reported that oxygen in liquid lead obeyed Henry's law over the entire oxygen concentration range. However, Charle and Osterwald [14] and Isecke [18] reported that the dissolution deviated from Henry's law. The values shown in Table 2 and Fig. 5 were calculated with respect to 1 at.% standard state on the basis of their data. The emf data obtained in the temperature range of 666–886 K for the saturated solution of oxygen in liquid lead and the Gibbs energy of formation PbO(s) derived

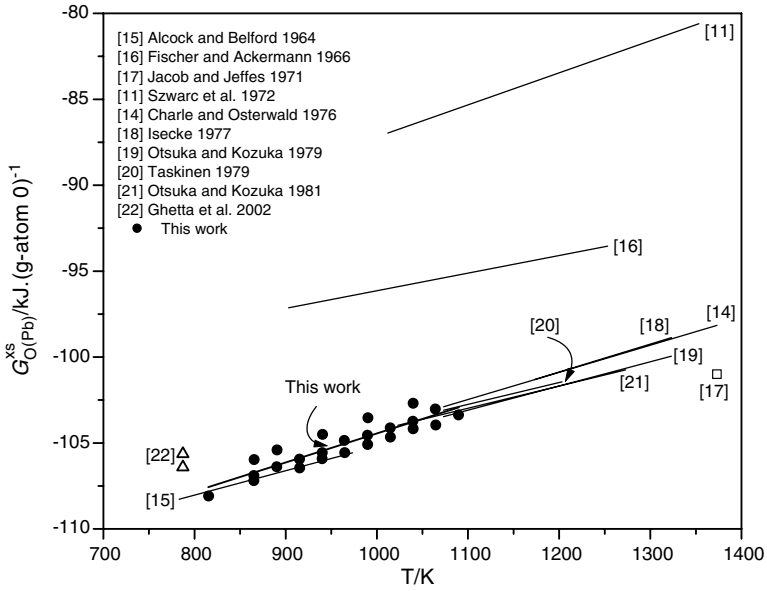

Fig. 5. Comparison of $G^{xs}_{O(Pb)}$ values from the present work with data reported in literature.

from it are in excellent agreement with our earlier data on this system [5].

Using the $G^{xs}_{O(Pb)}$ values measured in this work and standard Gibbs energy of formation of PbO(s) [5], the solubility of oxygen in liquid lead was derived and is given by

$$\log(S/\text{at.\%O}) = -5100/T + 4.32\ (\pm 0.04), \quad 815\text{–}1090\ \text{K}. \tag{21}$$

The derived solubility data are compared with the data reported in the literature [11,14,15,17,18,20,24] in Fig. 6. It is seen from the figure that the data from the present work are in agreement with the data reported by Alcock and Belford [15] and Taskinen et al. [20]. The present data on extrapolation to high temperatures are in close agreement with the data reported by Charle and Osterwald [14] and in good agreement with the data reported by Jacob

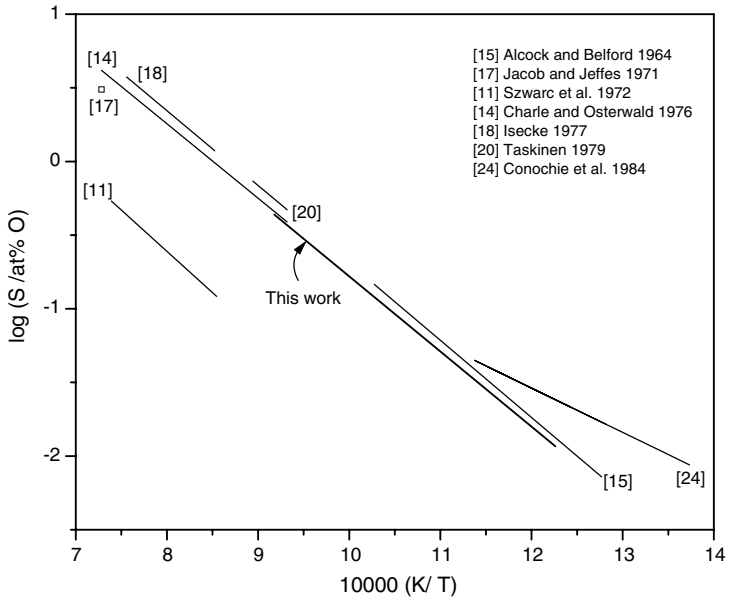

Fig. 6. Comparison of solubility of oxygen in lead derived from this work with data reported in the literature.

and Jeffes [17], Isecke [18] and Taskinen [20]. Conochie et al. [24] have used mild-steel containers for holding liquid Pb and have adopted an 'open top bubble' apparatus to determine the solubility. Their data are in agreement with the present data at high temperatures and deviate significantly at low temperatures. The reasons for the deviations at low temperatures are not clear but the existence of non-equilibrium conditions during their investigations at these temperatures is a distinct possibility. The data reported by Szwarc et al. [11] deviate from the rest of the data. As indicated earlier, use of chromel wire as electrical lead would have contributed to the deviation of the data reported by Szwarc et al. [11]. It is to be pointed out that the $G^{xs}_{O(Pb)}$ values reported by them also distinctly deviate from majority of the reported data.

4.2. Oxygen in liquid LBE

4.2.1. Diffusivity

The experimental parameters such as temperature, applied voltages and the derived diffusion coefficient of oxygen in LBE are summarised in Table 5. The typical plots of $\ln i_{ion}$ against time are shown in Fig. 7. The potential drop arising due to kinetics of oxygen ion transport across the electrolyte during these measurements was also found to lie between 0.5 and 1.5 mV. The temperature dependence of the diffusion coefficient of oxygen in liquid LBE is shown in Fig. 8 along with the linear least-squares fitted expression given below

Table 5
Experimental results of oxygen diffusion measurements in the LBE–O system

T (K)	E_1 (mV)	E_2 (mV)	D_O (cm^2 s^{-1})
810.5	672.3	872.3	4.29×10^{-6}
834.5	660.7	860.7	8.66×10^{-6}
910.1	733.1	933.1	1.99×10^{-5}
935.1	658.1	858.1	2.38×10^{-5}
959.6	630.6	830.6	2.20×10^{-5}
980.1	580.8	780.8	2.96×10^{-5}

$$\log(D_O^{LBE}/\text{cm}^2\ \text{s}^{-1}) = -0.813 - 3612/T\ (\pm 0.091),\quad 811\text{–}980\ \text{K}. \tag{22}$$

The present data are of first kind for the diffusivity of oxygen in LBE. The diffusion coefficient of oxygen in liquid lead derived from this work and the diffusion coefficient of oxygen in liquid bismuth reported by Fitzner [39] are also shown in the figure for comparison. The data reported by Lefhalm et al. [25] are compared in Fig. 8, though their data determined at 703 K exhibited a dependence on the different masses of LBE. The estimated data by

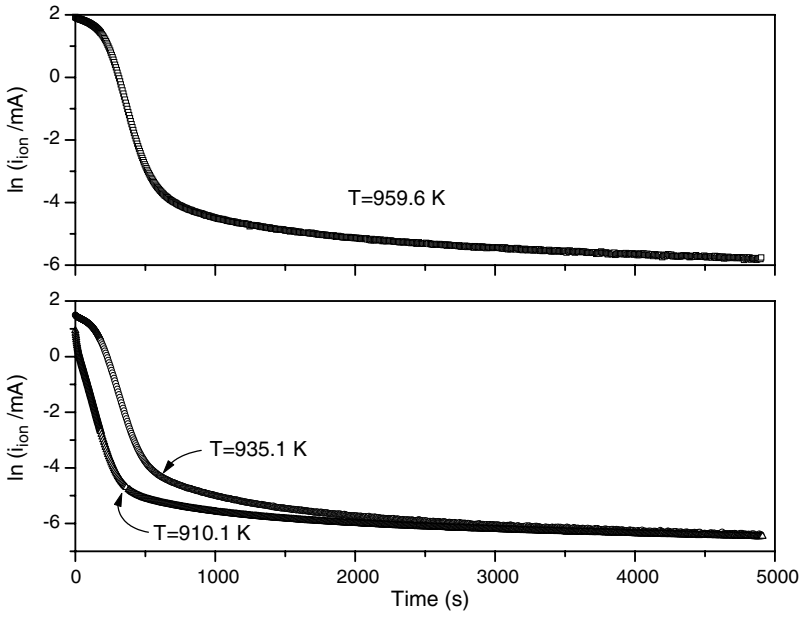

Fig. 7. Plots of $\ln i_{ion}$ vs. time derived using the measured cell current as a function of time during potentiostatic experiments in the LBE–O system at 959.6, 935.1 and 910.1 K.

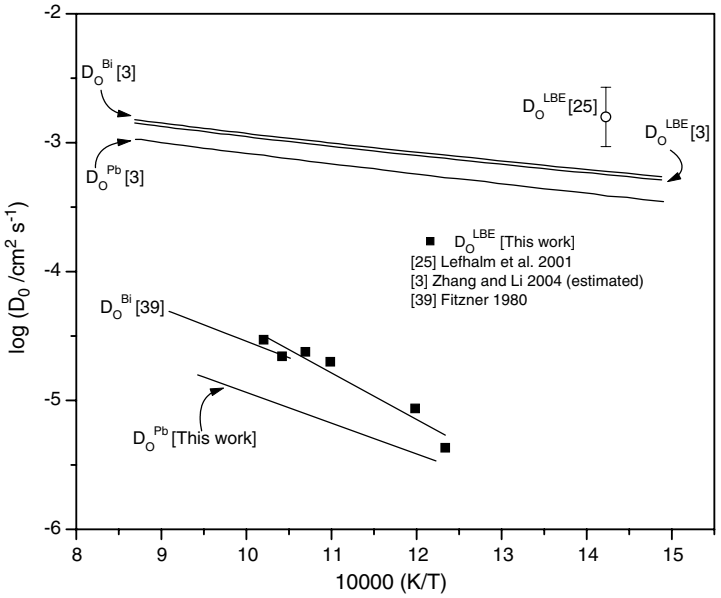

Fig. 8. Diffusion coefficient of oxygen in liquid LBE as a function of temperature. The data for liquid lead and bismuth are also shown for comparison.

Zhang and Li [3] are also shown although their estimation predicts higher values for the diffusion coefficient of oxygen in pure Pb and Bi than experimentally determined values. Their estimated values show that the diffusion coefficient of oxygen in LBE is slightly higher than the corresponding value in pure Pb but closer to that in pure Bi, in agreement to the trend observed in the present work.

4.2.2. Activity and solubility

The variation of the emf as a function of temperature for different concentrations of oxygen in liquid LBE is shown in Fig. 9. For each oxygen concentration, a distinct change in slope is seen at a specific temperature separating saturated and unsaturated regions. The oxygen partial pressure over LBE saturated with oxygen was derived from the emf data

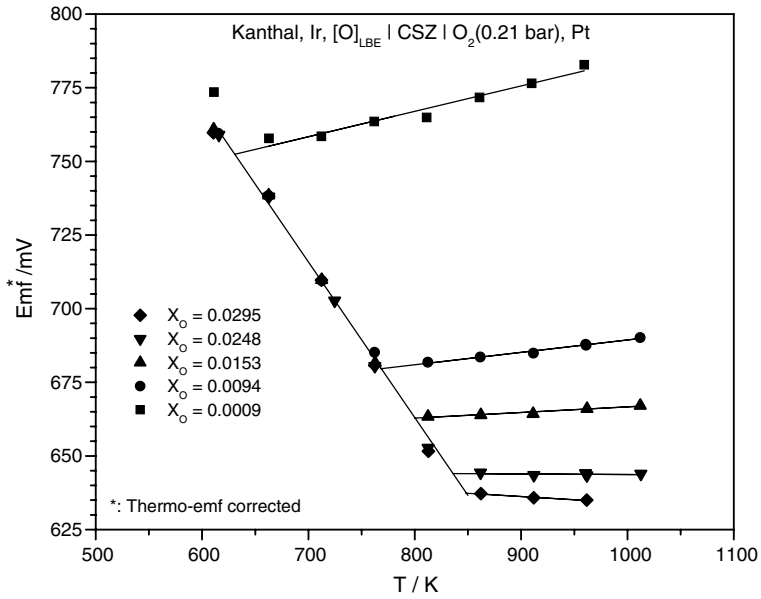

Fig. 9. Dependence of the emf on the cell temperature for different oxygen concentrations in liquid LBE.

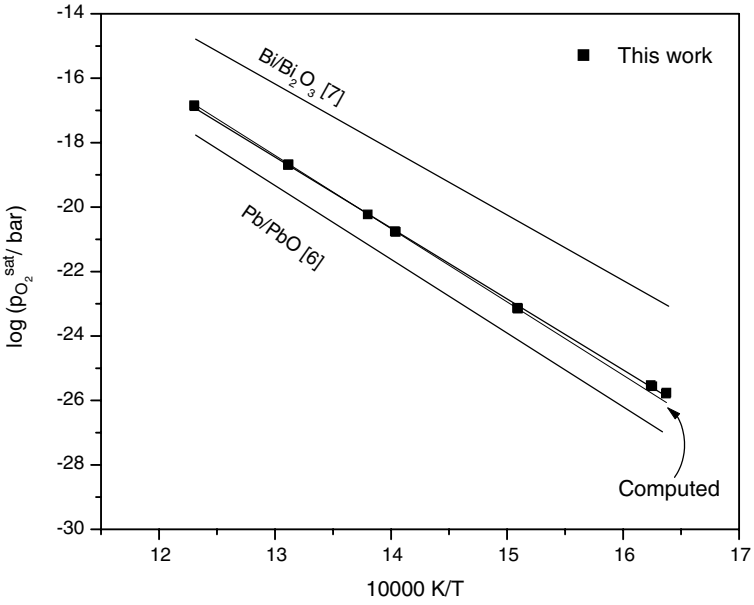

Fig. 10. Equilibrium oxygen partial pressure over LBE saturated with oxygen.

of the saturated region and is shown in Fig. 10. The least-squares fitted expression for $\log(p^{sat}_{O_2}/\text{bar})$ is given by

$$\log(p^{sat}_{O_2}/\text{bar}) = 10.15 - 22\,000/T \ (\pm 0.07), \quad 611\text{–}812\ \text{K}. \tag{23}$$

PbO(s) is generally assumed to be the oxide phase that precipitates from LBE on its saturation with oxygen, although it has not been unequivocally established by experiments. Assuming PbO(s) to be the precipitating phase, equilibrium oxygen potential of the following equilibrium as a function of temperature was computed:

$$[\text{Pb}]_{\text{LBE}} + 1/2\text{O}_2(\text{g}) = \text{PbO}(\text{s}).$$

Gibbs energy of formation of PbO(s) from Ref. [5] and data on the activity of Pb in LBE from Ref. [40] were used for this computation. These deduced data are also shown in Fig. 10, which are in excellent agreement with the oxygen potentials measured in the present work (Eq. (23)). This clearly indicates that the oxide in equilibrium with oxygen saturated LBE is PbO(s).

Using the emf data for the unsaturated solution of oxygen in liquid LBE, $G^{xs}_{O(LBE)}$ values with 1 at.% standard state were derived as a function of temperature and are shown in Fig. 11. The least-squares fitted expression for $G^{xs}_{O(LBE)}$ is given by,

$$G^{xs}_{O(LBE)} = -127398 + 27.938T \ (\pm 717)\text{J}(\text{g atom O})^{-1}, \quad 812\text{–}1012\ \text{K}. \tag{24}$$

These $G^{xs}_{O(LBE)}$ values are compared with the data available in the literature [26–28] in Fig. 11. The activity of oxygen in Pb–Bi alloys of different compositions had been measured in these works (see Section 2.2). The Gibbs energy of solution of oxygen in LBE (cf. LBE composition of 44.1 at.% Pb), was derived by interpolation of their data and used for this comparison. Though the data reported by Otsuka et al. [27] at 1173 K were for the Pb–Bi alloy with a composition of 45 at.% of Pb, they are also shown in the figure for comparison. Extrapolation of the data from the present work to high temperatures shows its fair agreement with the data reported by Taskinen [26] and Otsuka et al. [27]. The data reported by Anik and Frohberg [28] deviate significantly from the present data. These authors had used platinum as the electrical lead for the molten alloy. As mentioned in an earlier section, platinum is not compatible with Pb/Bi [38] and this could be the reason for the deviation. The data reported by Prabhakar and Kapoor [29] could not be compared as their measurements were for alloys with Bi concentration up to about 3 wt% only. It has to be pointed out that the present data for the activity of oxygen in LBE are of the first kind at

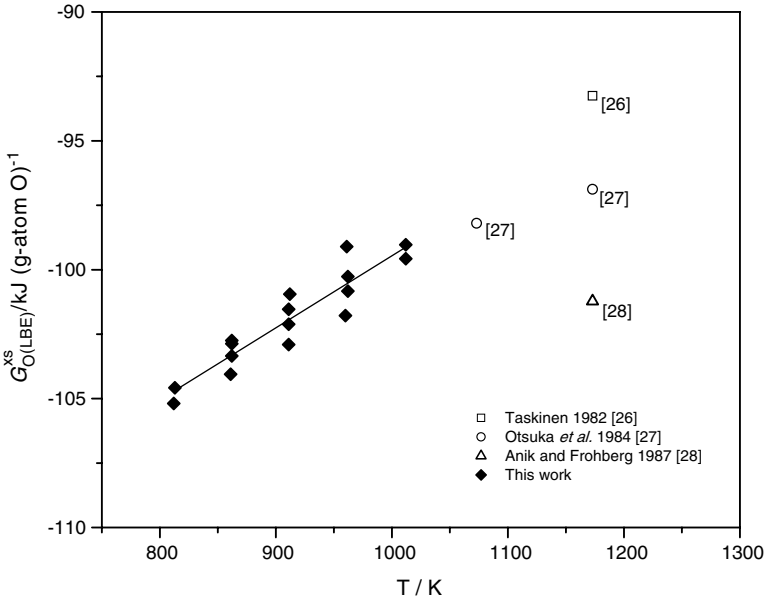

Fig. 11. Comparison of $G^{xs}_{O(LBE)}$ from present work with literature data.

low temperatures and they also cover a wide temperature range.

Using the $G^{xs}_{O(LBE)}$ values and measured equilibrium oxygen pressures under oxygen saturated conditions, the solubility of oxygen in liquid LBE was derived and is given by the following expression:

$$\log(S/\text{at.\%O}) = -4287/T + 3.53\ (\pm 0.06), \quad 812\text{–}1012\ \text{K}. \tag{25}$$

Fig. 12 compares the solubility data from the present work with the data reported in the literature [30–33]. The data reported by Gromov et al. [30] exhibit a

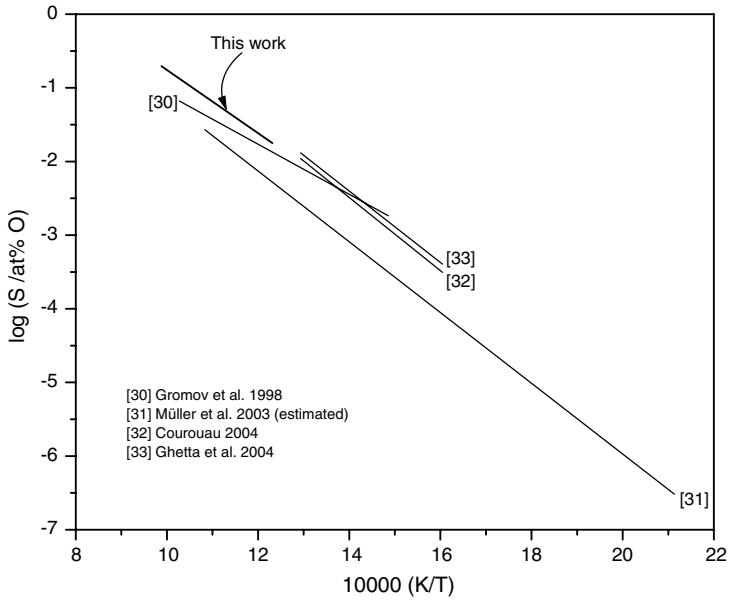

Fig. 12. Comparison of the solubility of oxygen in LBE derived from this work with literature data.

lower slope compared to all other data including that of present work. It can be seen from the figure that the present data on extrapolation to lower temperatures are in good agreement with the data reported by Courouau [32] and Ghetta et al. [33]. Courouau [32] derived the solubility expression using the emf data from several oxygen sensors operated in LBE. From the emf obtained in oxygen-unsaturated LBE, the dissolved oxygen concentration was derived by assuming Henry's law and by employing solubility data reported by Gromov et al. (Orlov's expression) [30]. By studying the temperature dependence of the emf of such a cell, the temperature at which LBE got saturated with oxygen was deduced. This was repeated with several oxygen sensors with LBE containing different concentrations of oxygen. The data obtained were used to recalculate the oxygen solubility data. By this approach, one would expect to get back the solubility expression reported by Gromov et al. [30] with uncertainties owing to sensor-to-sensor variations and experimental uncertainties such as difficulties in maintaining a constant oxygen concentration during the measurement as mentioned by the author himself [32,41]. In fact, solubility data reported by Courouau [32] show only a small deviation from data reported by Gromov et al. [30] although a deviation in slope is observed. Müller et al. [31] had estimated the solubility of oxygen in LBE from the corresponding binary data and as seen from the figure, these estimated values differ significantly from the rest of the data.

5. Conclusions

Diffusivity, activity and solubility of oxygen in liquid lead and LBE were measured and compared with available literature data. Discrepancies among the literature data on the diffusivity of oxygen in liquid lead and possible causes for the discrepancies were brought out. The present data on diffusivity of oxygen in lead are of first kind at low temperatures down to 818 K. The activity of oxygen in LBE at low temperatures and the diffusivity of oxygen in LBE have been determined for the first time. The solubility of oxygen in LBE at temperatures up to 1012 K have also been determined.

Acknowledgements

The authors sincerely acknowledge Mrs. Kitheri Joseph, Liquid Metals and Structural Chemistry Division for her help in DTA analysis. The authors acknowledge Dr. G. Periaswami, Head, Materials Chemistry Division, IGCAR for his constant encouragement during this work.

References

[1] B.F. Gromov (Ed. in chief), Proceedings of Heavy Liquid Metal Coolants in Nuclear Technology (HLMC-98), vol. 1 and 2, SSC RF-IPPE, Obninsk, 1999.
[2] B.F. Gromov, G.I. Toshinsky, V.V. Checkunov, Yu.I. Orlov, Yu.S. Belomytsev, I.N. Gorelov, A.G. Karabash, M.P. Leonchuk, D.V. Pankratov, Yu.G. Pahkin, in: B.F. Gromov (Ed. in chief), Proceedings of Heavy Liquid Metal Coolants in Nuclear Technology (HLMC-98), vol. 1, SSC RF-IPPE, Obninsk, 1999, p. 14.
[3] J. Zhang, N. Li, Review of studies on fundamental issues in LBE corrosion, Los Alamos National Laboratory, LA-UR-04-0869, 2004.
[4] G. Müller, G. Schumacher, F. Zimmermann, J. Nucl. Mater. 278 (2000) 85.
[5] R. Ganesan, T. Gnanasekaran, Raman S. Srinivasa, J. Nucl. Mater. 320 (2003) 258.
[6] R. Ganesan, T. Gnanasekaran, Raman S. Srinivasa, J. Chem. Thermodynam. 35 (2003) 1703.
[7] R. Ganesan, T. Gnanasekaran, Raman S. Srinivasa, Behaviour of oxygen in lead–bismuth alloy, TOFA 2004 – Discussion Meeting on Thermodynamics of Alloys, Vienna, Austria, 2004.
[8] F.G. Arcella, G.R. Fitterer, J. Metals 47A (1968).
[9] G.K. Bandyopadhyay, H.S. Ray, Metall. Trans. 2 (1971) 3055.
[10] S. Honma, N. Sano, Y. Matsushita, Metall. Trans. 2 (1971) 1494.
[11] R. Szwarc, K.E. Oberg, R.A. Rapp, High Temp. Sci. 4 (1972) 347.
[12] M. Kawakami, M. Goto, J. Iron Steel Inst. Japan 59 (1973) 196.
[13] S. Otsuka, Z. Kozuka, Metall. Trans. 6B (1975) 389.
[14] H. Charle, J. Osterwald, Z. Phys. Chem. NF 99 (1976) 199.
[15] C.B. Alcock, T.N. Belford, Trans. Faraday Soc. 60 (1964) 822.
[16] W.A. Fischer, W. Ackermann, Arch. Eisenhüttenw. 37 (1966) 43.
[17] K.T. Jacob, J.H.E. Jeffes, Trans. Inst. Miner. Metall. 80 (1971) C32.
[18] B. Isecke, Equilibria study in the bismuth–, antimony–, and lead–oxygen systems, Dissertation, TU Berlin, 1977.
[19] S. Otsuka, Z. Kozuka, Metall. Trans. 10B (1979) 565.
[20] A. Taskinen, Scand. J. Metall. 8 (1979) 185.
[21] S. Otsuka, Z. Kozuka, Metall. Trans. 12B (1981) 616.
[22] V. Ghetta, J. Fouletier, M. Henault, A. Le Moulec, J. Phys. IV France 12 (2002) 123.
[23] D. Risold, J.-I. Nagata, R.O. Suzuki, J. Phase Equilibria 19 (1998) 213.
[24] D.S. Conochie, C. Ebiogwu, D.G.C. Robertson, Trans. Inst. Miner. Metall. C93 (1984) C45.
[25] C.H. Lefhalm, J.U. Knebel, K.J. Mack, J. Nucl. Mater. 296 (2001) 301.
[26] A. Taskinen, Z. Metall. 73 (1982) 163.
[27] S. Otsuka, Y. Kurose, Z. Kozuka, Metall. Trans. 15B (1984) 141.

[28] S. Anik, M.G. Frohberg, Ber. Bunsenges. Phys. Chem. 91 (1987) 790.
[29] S.R. Prabhakar, M.L. Kapoor, Aust. Inst. Miner. Met. Proc. 1 (1995) 85.
[30] B.F. Gromov, Yu.I. Orlov, P.N. Martynov, V.A. Gulevsky, in: B.F. Gromov (Ed. in chief), Proceedings of Heavy Liquid Metal Coolants in Nuclear Technology (HLMC-98), vol. 1, SSC RF-IPPE, Obninsk, 1999, p. 87.
[31] G. Müller, A. Heinzel, G. Schumacher, A. Weisenburger, J. Nucl. Mater. 321 (2003) 256.
[32] J.-L. Courouau, J. Nucl. Mater. 335 (2004) 254.
[33] V. Ghetta, A. Maitre, J.-C. Gachon, in: Proceedings of the MEGAPIE Technical Review Meeting, 24–26 May 2004, SUBATECH, Nantes, France (as cited in Ref. [32]).
[34] T.A. Ramanarayanan, R.A. Rapp, Metall. Trans. 3 (1972) 3239.
[35] K. Oberg, L.M. Friedman, W.M. Boorstein, R.A. Rapp, Metall. Trans. 4 (1973) 61.
[36] H. Sato, in: S. Geller (Ed.), Solid Electrolytes, Springer, Berlin, 1977, p. 3.
[37] J. Crank, The Mathematics of Diffusion, Oxford Press, 1957.
[38] T.B. Massalski (Ed.), Binary Alloys Phase Diagrams, 2nd ed., The Materials Information Society, USA, 1990.
[39] K. Fitzner, Thermochim. Acta 35 (1980) 277.
[40] N.A. Gokcen, J. Phase Equilibria 13 (1992) 21.
[41] J.-L. Courouau, P. Deloffre, R. Adriano, J. Phys. IV France 12 (2002) 141.